Revue des Energies Renouvelables Vol. 20 N°4 (2017) 541 - 553
DOI: https://doi.org/10.54966/jreen.v20i4.648

Comparative study of two steam reforming kinetic models for pure hydrogen production from ethanol in a separating reactor

Imene Ziani and Lemnouer Chibane *

Laboratoire de Génie des Procédés Chimiques, LGPC
Département de Génie des Procédés, Faculté de Technologie
Université Ferhat Abbas, Sétif 1, Algérie

(reçu le 10 Octobre 2017 - accepté le 15 Décembre 2017)

Abstract - *The present work deal with a comparative study of two kinetics models of ethanol conversion by steam reforming for pure hydrogen generation in a Pd-Ag based membrane reactor. For this purpose, a mathematical model describing the reaction and separation phenomena that take place simultaneously in the membrane reactor was developed. The numerical solution of the set of differential equations constituting the obtained model allows us to quantify the process performance over both Ni/Mg-Al, and Ni//γAl_2O_3 catalysts. According to the obtained results, it was found that the performance of the ethanol steam reforming process depends strongly on the catalyst nature. In addition, the process's strongly sensitive to the used operating conditions, especially hydrogen partial pressure in permeate and in reaction sides, in which a good correlation and a synergistic effect between these parameters could be established. Under the optimal operating conditions, the quantity of hydrogen recovered when using the Ni/Al_2O_3 is three times greater than that obtained by using the Ni/Mg-Al catalyst.*

Résumé - *Le présent travail porte sur une étude comparative de deux modèles cinétiques de conversion de l'éthanol par réformage à la vapeur d'eau pour la production d'hydrogène pur dans un réacteur membranaire à base de Pd-Ag. Pour cet objectif, un modèle mathématique décrivant les phénomènes de réaction et de séparation qui ont eu lieu simultanément dans le réacteur membranaire est développé. La solution numérique de l'ensemble des équations différentielles constituant le modèle mathématique obtenu nous permet de quantifier les performances du procédé sur deux types de catalyseurs à base de Ni/Mg-Al, et à base de Ni//γAl_2O_3. Selon les résultats obtenus, on constate que les performances du procédé de vaporeformage de l'éthanol dépendent fortement de la nature du catalyseur utilisé. En outre, le procédé est fortement sensible aux conditions opératoires utilisées, notamment la pression partielle de l'hydrogène dans la zone de perméat et de réaction, dans laquelle une bonne corrélation et un effet synergique entre ces paramètres pourraient être établis. Sous certaines conditions de fonctionnement optimales, la quantité d'hydrogène récupérée lors de l'utilisation du Ni/Al_2O_3 est trois fois supérieure à celle obtenue lorsqu'en utilisant le catalyseur Ni/Mg-Al.*

Keywords: Membrane reactor - Hydrogen production - Pure hydrogen recovery - Ethanol conversion - Steam reforming - Nickel based catalysts.

1. INTRODUCTION

Nowadays, the environmental issues become more important and crucial for our society and so they constitute one of the priorities of governments. The air pollution caused primarily by the automobiles exhaust is one among the major problems that must be resolved definitely and immediately. The best solution is to find an alternative fuel that reduces air pollution and does not contribute to the greenhouse effect. Hydrogen is the fuel that meets these particular ecological requirements and this by the use of the fuel cell in which produces electricity and releases only water [1].

Several routes and sources are possible to produce it [2]. However, to produce pure hydrogen with a lower cost and with quantities that could replace fossil hydrocarbons,

* lchibane@yahoo.com

some actions are considered for producing hydrogen from renewable feedstock for example. Therefore, many studies are aimed to generate hydrogen from methanol [3] or from ethanol [4, 5], since it can be produced in large quantities from various biomass sources [6, 7] and therefore, it does not increases the greenhouse effect.

In addition due to its low production cost, its relatively high hydrogen content and its availability, ethanol is a promising fuel for the production of hydrogen [8, 9] by various chemical routes among which the most used in industry are: decomposition [10], steam reforming [11], partial oxidation and oxidative steam reforming [12]. The catalytic steam reforming appears as the best alternative seen the many environmental benefits it offers.

Indeed, this method is currently considered the most promising in the field of hydrogen production for fuel cells [13]. The Ethanol Steam Reforming, 'ESR' process's a fairly complex process of chemical point of view. The ethanol steam reforming reaction {Eq.(1)} is the main reaction of this process. It is endothermic, irreversible at high temperatures and requires an external energy supply [14]. Reaction given by {Eq.(2)} is an exothermic reaction called water gas shift reaction. The thermal decomposition reaction of ethanol is given by {Eq.(3)} [15].

These reactions are not the only ones occurring. Indeed, they are accompanied by a large number of reactions that coexist in equilibrium. The main products of ethanol steam reforming, 'ESR' are H_2, CO_2, CO and CH_4. They are formed mainly by the following reactions [15]:

$$C_2H_5OH + 3\,H_2O \rightarrow 2\,CO_2 + 6\,H_2O \quad (1)$$

$$CO + H_2O \rightarrow CO_2 + H_2 \quad (2)$$

$$C_2H_5OH \rightarrow CO + CH_4 + H_2 \quad (3)$$

However, depending on the catalyst nature and on operating conditions, other reactions may also take place [16].

$$C_2H_5OH \rightarrow CH_3CHO + H_2O \quad (4)$$

$$C_2H_5OH \rightarrow C_2H_4 + H_2O \quad (5)$$

$$C_2H_5OH + H_2O \rightarrow 2\,CO + 4\,H_2O \quad (6)$$

$$C_2H_5OH + H_2O \rightarrow 2\,CO + 4\,H_2 \quad (7)$$

$$2\,C_2H_5OH + 2\,H_2 \rightarrow (C_2H_5)_2 + H_2O \quad (8)$$

$$C_2H_5OH + H_2O \rightarrow CH_3COOH + 2\,H_2 \quad (9)$$

$$CH_3CHO \rightarrow CH_4 + CO \quad (10)$$

$$2\,CH_3CHO \rightarrow CH_3COCH_3 + CO + H_2 \quad (11)$$

$$CO + 3\,H_2 \rightarrow CH_4 + H_2O \quad (12)$$

$$C_2H_4 \rightarrow C \quad (13)$$

$$CH_4 + 2\,H_2O \rightarrow CO_2 + 4\,H_2 \quad (14)$$

$$CH_4 \rightarrow C + 2\,H_2 \quad (15)$$

$$2\,CO \rightarrow CO_2 + C \quad (16)$$

The present work consists of a simulation study which is focused on the comparison of two kinetic models of ethanol steam reforming, 'ESR' [17, 18] for pure hydrogen production in a Pd-Ag membrane reactor.

A parametric sensitivity analysis was also done to establish the possible relationship between the key operating conditions over both kinetic models.

2. MATHEMATICAL MODEL

2.1 Reactor description

In this work, a packed bed reactor integrated a H_2-permselective Pd-Ag based membrane as shown in figure 1 was used for ESR, in which the reactions occur in the inner tube (reaction zone).The hydrogen produced diffuse from the inner tube through the membrane to the space between the two concentric tubes (permeation side).

Therefore, the hydrogen can be recovered in the permeate side separately from the other products. In this zone, an inert sweep gas is used (nitrogen) to evacuate the hydrogen. The reactor dimensions [15] and the other operating conditions used in this study are recapitulated in **Table 1**.

To reduce the complexity of the mathematical model development and its solution, only the reactions with significant rates will be considered, and the following assumptions are incorporated:

- The whole system may be considered isothermal and isobaric, - The plug flow model is assumed for the reaction and permeation sides in steady state conditions,- Ideal gas law is applicable,- The catalyst deactivation by coke formation is negligible,-The membrane is only permeable to hydrogen and has an infinite selectivity to hydrogen.

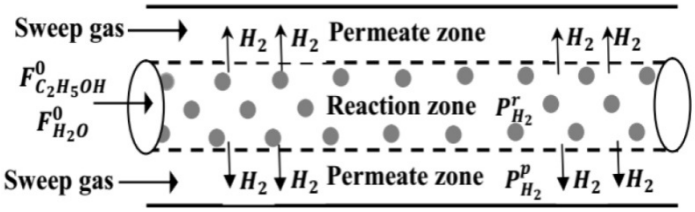

Fig. 1: Schematic diagram of membrane reactor

Table 1: Reactor dimension and operating conditions used for simulation

Parameter	Value
Reactor length, Z	0.2 m
Internal reactor diameter, D_i	10^{-2} m
Catalyst weight, W	$8.72\text{x}10^{-5}$ kg
Ethanol inlet molar flow rate, F^0_{C2H5OH}	$5.16\text{x}10^{-6}$ mol s^{-1}
Membrane thickness, δ	$2\text{x}10^{-5}$ m
Membrane activation energy, E_p	$29.16\text{x}10^{+3}$ J mol^{-1}
Temperature, T	550-650K
Inlet feed ratio (steam/ethanol), α	1-4
Total pressure in reaction zone, P_p	0.7-1.5Pa
Total pressure in permeate zone, P_t	1-0.1Pa
Sweeping ratio (sweep gas/ethanol), I	2-5

2.2 Reaction schemes and kinetics models

a) Case of Ni/Mg-Al catalyst (model: m1)

The main products of the ethanol steam reforming reaction over Ni/Mg-Al catalyst according to Langmuir - Hinshelwood model [17] are: H_2, CO_2, CO, CH_3CHO and CH_4. They are formed mainly through the following reactions summarized in **Table 2**.

Table 2: Reaction scheme of ESR over Ni/Mg-Al catalyst

Reaction		$\Delta H_{298K}(kJmol^{-1})$	
Ethanol dehydrogenation	$CH_3CH_2OH \leftrightarrow CH_3CHO + H_2$	+68.4	(17)
Acetaldehyde decomposition	$CH_3CHO \leftrightarrow CH_4 + CO$	-18.8	(18)
Methane steam reforming	$CH_4 + H_2O \leftrightarrow CO + 3H_2$	+205.9	(19)
Water gas shift	$CO + H_2O \leftrightarrow CO_2 + H_2$	-41	(20)
Overall reaction	$CH_3CH_2OH + 3H_2O \leftrightarrow 2CO_2 + 6H_2$	+172.7	(21)

The rate expressions of reactions (17, 18, 19 and 20) are as follows:

$$r_1^{m1} = k_1 Y_{C_2H_5OH}\left(1 - \frac{1}{K_1}\frac{Y_{CH_3CHO}\, Y_{H_2}}{Y_{C_2H_5OH}}\right)\left(\frac{1}{DEN}\right) \tag{22}$$

$$r_2^{m1} = k_2 Y_{CH_3CHO}\left(1 - \frac{1}{K_2}\frac{Y_{CO}\, Y_{H_2}}{Y_{C_2H_5OH}}\right)\left(\frac{1}{DEN}\right) \tag{23}$$

$$r_3^{m1} = k_3 Y_{CH_4}\, Y_{H_2O}\left(1 - \frac{1}{K_3}\frac{Y_{CO}\, Y_{H_2}^3}{Y_{CH_4}\, Y_{H_2O}}\right)\left(\frac{1}{DEN^2}\right) \tag{24}$$

$$r_4^{m1} = k_4 Y_{CO}\, Y_{H_2O}\left(1 - \frac{1}{K_4}\frac{Y_{CO_2}\, Y_{H_2}}{Y_{CO}\, Y_{H_2O}}\right)\left(\frac{1}{DEN^2}\right) \tag{25}$$

$$\begin{aligned} DEN = {} & 1 + K_{C_2H_5OH} Y_{C_2H_5OH} + K_{H_2O} Y_{H_2O} + K_{CH_4} Y_{CH_4} \\ & + K_{OH} Y_{H_2O} \Big/ Y_{H_2}^{0.5} + K_{CH_3} Y_{CH_4} \Big/ Y_{H_2}^{0.5} + K_{CO} Y_{CO} + K_H Y_{H_2}^{0.5} \end{aligned} \tag{26}$$

Here, $Y_{C_2H_5OH}$, Y_{CO}, Y_{CO_2}, Y_{CH_4}, Y_{CH_3CHO} and Y_{H_2} are the molar fractions.

The Arrhenius and adsorption constants are given as follows, respectively:

$$k_i(T) = k_i^0 \exp\left(-\frac{E_i}{RT}\right) \tag{27}$$

$$k_i(T) = k_j^*(673.15\ K) \exp\left(-\frac{\Delta H_j}{R}\left(\frac{1}{T} - \frac{1}{673.15}\right)\right) \tag{28}$$

ΔH_j is the heat of reaction, E_i is the activation energy and R is the universal gas constant=8.314 J/m.K.

The pre-exponential factors of {Eq. 27} and {Eq. 28}, activation energy and enthalpies are summarized in **Table 3**.

Table 3: Kinetic parameters of ESR over Ni/Mg-Alcatalyst [17]

Rate constants	$k_i^0\ (molkg^{-1}s^{-1})$	$E_{Ai}\ (kJmol^{-1})$
k_1	$(1.14 \pm 0.16)x10^{4}$	31.8 ± 3.6
k_2	$(8.42 \pm 1.03)x10^{3}$	24.8 ± 2.5
k_3	$(9.87 \pm 1.59)x10^{9}$	119 ± 8.9
k_4	$(1.06 \pm 0.13)x10^{9}$	60.4 ± 4.4
Adsorption constants	$k_j^*\ (molkg^{-1}s^{-1})$	$\Delta H_j\ (kJmol^{-1})$
$K^*_{C_2H_5OH}$	$(9.83 \pm 0.56)x10^{0}$	-4.96 ± 0.52
$K^*_{H_2O}$	$(1.32 \pm 0.11)x10^{-1}$	-56.8 ± 3.16
$K^*_{CH_4}$	$(1.12 \pm 0.23)x10^{2}$	-66.8 ± 4.59
K^*_{OH}	$(1.73 \pm 0.16)x10^{-2}$	-53.5 ± 3.49
$K^*_{CH_3}$	$(1.07 \pm 0.20)x10^{-3}$	-66.7 ± 6.82
K^*_{H}	$(7.35 \pm 1.02)x10^{-7}$	-27.1 ± 1.22
K^*_{CO}	$(1.48 \pm 0.26)x10^{-2}$	-79.5 ± 8.21

b) Case of Ni/Al_2O_3 catalyst (model: m2)

When the reaction was performed over Ni/Al_2O_3 catalyst, the main products according to the reaction scheme as presented in **Table 4** are H_2, CO_2, CO and CH_4.

Table 4: Reaction scheme of ESR over Ni/γAl_2O_3catalyst [18]

Reaction	$\Delta H_{298K}(kJ\ mol^{-1})$		
Ethanol decomposition	$CH_3CH_2OH \rightarrow CH_4 + CO + H_2$	+49	(29)
Water gas shift	$CO + H_2O \leftrightarrow CO_2 + H_2$	-41.4	(30)
Methane steam reforming	$CH_4 + H_2O \leftrightarrow CO + 3H_2$	+205.9	(31)
Sum of (30) and (31)	$CH_4 + 2H_2O \leftrightarrow CO_2 + 4H_2$	+165	(32)

The corresponding rate expressions of reactions (29, 30, 31 and 32) are given below and the different kinetic parameters are presented in **Table 5**.

$$r_1^{m2} = k_1 P_t Y_{C_2H_5OH} \tag{33}$$

$$r_2^{m2} = \frac{k_2 P_t}{Y_{H_2} DEN^2}\left(Y_{CO}\ Y_{H_2O} - \frac{Y_{CO_2}\ Y_{H_2}}{K_2} \right) \tag{34}$$

$$r_3^{m2} = \frac{k_3 P_t^{-0.5}}{Y_{H_2}^{2.5} DEN^2}\left(Y_{CH_4}\ Y_{H_2O} - \frac{Y_{CH_4}\ Y_{H_2}^3}{K_3} P_t^2 \right) \tag{35}$$

$$r_4^{m2} = \frac{k_4 P_t^{-0.5}}{Y_{H_2}^{3.5} DEN^2}\left(Y_{CH_4}\ Y_{H_2O} - \frac{Y_{CO_2}\ Y_{4_2}^3}{K_4} P_t^2 \right) \tag{36}$$

$$DEN = 1 + P_t.\left(K^*_{CO}\ Y_{CO} + K^{\mu}_{H_2}\ Y_{H_2} + K^{\mu}_{CH_4}\ Y_{CH_4} \right) + \frac{K^*_{H_2O}\ Y_{H_2O}}{Y_{H_2}} \tag{37}$$

$Y_{C_2H_5OH}$, Y_{CO}, Y_{CO_2}, Y_{CH_4}, Y_{H_2O} and Y_{H_2} are the molar fractions.

Table 5: Kinetic and adsorption parameters of ESR over Ni/γAl_2O_3catalyst [18]

Rate constants	
$k_1\ (molPa^{-1}g_{cat}^{-1}s^{-1})$	$\frac{4.55x10^{-5}}{T}\exp\left(-\frac{2030}{T}\right)$
$k_2(molPa^{-1}g_{cat}^{-1}s^{-1})$	$5.43x10^{-3}\exp\left(-\frac{8074.33}{T}\right)$
$k_3\ (molPa^{0.5}g_{cat}^{-1}s^{-1})$	$3.711x10^{14}\exp\left(-\frac{28879}{T}\right)$
$k_4\ (molPa^{0.5}g_{cat}^{-1}s^{-1})$	$8.960x10^{13}\exp\left(-\frac{29336.1}{T}\right)$
Equilibrium constants	
$K_2(Pa^0)$	$\exp\left(\frac{4400}{T}-4.036\right)$
$K_3(Pa^2)$	$1x10^{10}\exp\left(-\frac{26830}{T}+30.114\right)$
$K_4(Pa^2)$	K_2K_3
Adsorption constants	
$K_{CO}^{*}(Pa^{-1})$	$8.230x10^{-10}\exp\left(\frac{8497.71}{T}\right)$
$K_{CH_4}^{*}(Pa^{-1})$	$6.640x10^{-9}\exp\left(\frac{4604.28}{T}\right)$
$K_{H_2}^{*}(Pa^{-1})$	$6.120x10^{-14}\exp\left(\frac{9971.13}{T}\right)$
$K_{H_2O}^{*}(Pa^0)$	$1.770x10^{+5}\exp\left(-\frac{10666.35}{T}\right)$

2.3 Mole balance

The following measurements are used as metrics to quantify the reactor performance:

■ Ethanol conversion

$$X_{C_2H_5OH} = \frac{F^0_{C_2H_5OH} - F_{C_2H_5OH}}{F^0_{C_2H_5OH}} \tag{38}$$

■ Hydrogen protection

$$X_{H_2} = \frac{F_{H_2}}{F^0_{C_2H_5OH}} \tag{39}$$

■ Hydrogen recover

$$Y_{H_2} = \frac{F^P_{H_2}}{F^0_{C_2H_5OH}} \tag{40}$$

The axial differential mass balance in the gaseous phase in terms of molar flow rates is given for each chemical species by the expressions.

$$\frac{dF_i}{dz} = \rho A \sum \upsilon_{ij} r_i - \frac{dF_i^p}{dz} \tag{41}$$

$$\frac{dF_i^p}{dz} = \begin{cases} = 0 \text{ for } i = C_2H_5OH,\ H_2O,\ CH_3CHO,\ CH_4,\ CO \text{ and } CO_2 \\ \neq 0 \text{ for } i = H_2 \end{cases} \tag{42}$$

υ_{ij}, is the stoichiometric coefficient, ρ, is the catalyst density (kg/m^3) and A is the reactor section (m^2).

In the other hand, according to definition given by {Eq. (40)}, the permeated hydrogen can be written as follows:

$$\frac{dF_{H_2}^p}{dz} = F_{C_2H_5OH}^0 \frac{dY_{H_2}}{dz} \tag{43}$$

By introducing the above metrics, the ethanol conversion and the produced hydrogen over Ni/Mg-Al (model:m1) are given as follows.

$$\frac{dX_{C_2H_5OH}}{dz} = \frac{\rho A}{F_{C_2H_5OH}^0} r_1^{m1} \tag{44}$$

$$\frac{dX_{H_2}}{dz} = \frac{\rho A}{F_{C_2H_5OH}^0} \left(r_1^{m1} + 3r_3^{m2} + r_4^{m1} \right) - \frac{dY_{H_2}}{dz} \tag{45}$$

In the case of Ni/Al_2O_3 catalyst (model: m2), the following expressions can be written:

$$\frac{dX_{C_2H_5OH}}{dz} = \frac{\rho A}{F_{C_2H_5OH}^0} r_1^{m2} \tag{46}$$

$$\frac{dX_{H_2}}{dz} = \frac{\rho A}{F_{C_2H_5OH}^0} \left(r_1^{m2} + r_2^{m2} + 3r_3^{m2} + 4r_4^{m2} \right) - \frac{dY_{H_2}}{dz} \tag{47}$$

The hydrogen recovery for both kinetic models (Y_{H_2}) is calculated through the following equation obtained from the mole balance in permeation side.

$$\frac{dY_{H_2}}{dz} = D_0 \frac{\pi D_i}{\delta F_{C_2H_5OH}^0} \left(\sqrt{P_{H_2}^r} - \sqrt{P_{H_2}^p} \right) \exp\left(-\frac{E_p}{R T} \right) \tag{48}$$

D_0, is the permeation coefficient of hydrogen (mol.m/m^2.s.Pa$^{-0.5}$).

The hydrogen partial pressure en permeate zone is given by:

$$P_{H_2}^p = \frac{Y_{H_2}^p P_p}{Y_{H_2}^p + I} \tag{49}$$

The sweeping gas ratio (I) is defined as the ration between the molar flow rates of sweep gas to the inlet ethanol molar flow rate.

$$I = \frac{F_I}{F_{C_2H_5OH}^0} \tag{50}$$

$P_{H_2}^r$, is the hydrogen partial pressure in reaction zone calculated as follows.

$$P_{H_2}^r = \frac{F_{H_2}}{F_T} P_t \tag{51}$$

and

$$F_T = \sum F_i \tag{52}$$

i = C_2H_5OH, H_2O, CH_3CHO, CH_4, CO, H_2 and CO_2 for the first model m1 and i = C_2H_5OH, H_2O, CH_4, CO, H_2 and CO_2 for the second model m+2.

After introducing a dimensionless reactor length, the integration of the above set first order differential equations (44 - 48) along the axial direction was obtained by means of a fourth order Runge-Kutta routine with the initial conditions at the reactor inlet: $X_{C_2H_5OH}=0$, $X_{H_2}=0$ and $Y_{H_2}=0$.

Considering for each kinetic the allowable ranges of temperatures, the process performance is measured through the hydrogen production in reaction side and the pure hydrogen generated in the permeation side as principals metrics**.**

4. RESULTS AND DISCUSSION

In this work, a parametric sensitivity analysis was done by studying the effect of the key inputs on ethanol steam reforming, 'ESR' performance using two distinct kinetic models. The studied parameters were: temperature (T), inlet feed ratio (α), total pressure in reaction side (P_t), pressure in permeate side (P_p) and the sweeping gas ratio (I).

In first, the main results relative to the effect of temperature on ethanol steam reforming performance show that for the two kinetic models, the hydrogen production in the reaction zone increases with temperature increasing (figure 2**a** and figure 3**a**). This can be attributed for the first kinetic model to the endothermic nature of the ethanol dehydrogenation reaction {Eq.17}.

It should be noted that the hydrogen being produced *via* the endothermic methane steam reforming reaction {Eq.19} and *via* the exothermic water gas shift reaction {Eq.20}. But for the second kinetic model, the hydrogen production increase can be due to the improving in ethanol conversion achieved with increasing temperatures, especially by the endothermic ethanol decomposition reaction {Eq.29}. Both of the steam reforming reactions of methane {Eq.31} and {Eq.32} are also favorable.

In the other hand, it was found that for the first kinetic model, the production of hydrogen in the reaction zone is being directly proportional to the molar inlet feed ratio (steam to ethanol molar ratio). This effect is probably due to the fact that the increase of the steam promotes the forward direction of methane steam reforming reaction {Eq.19} and of water gas shift reaction {Eq.20}. For the second kinetic model, a slight variation of hydrogen production in the reaction zone was observed.

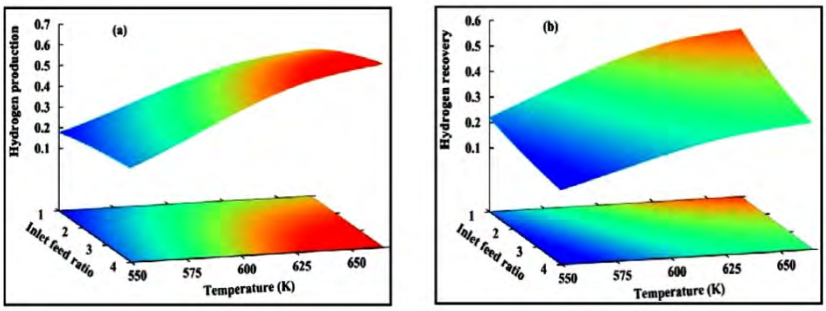

Fig. 2: Effect of temperature and the initial charge ratio on hydrogen production (**a**) and on pure hydrogen recovery (**b**) with Ni/Mg-Al kinetic model

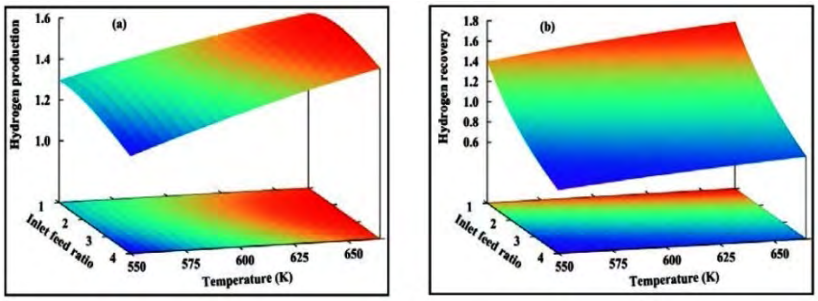

Fig. 3: Effect of temperature and the initial charge ratio on hydrogen production (**a**) and on pure hydrogen recovery (**b**) with Ni/Al_2O_3 kinetic model

The amount of hydrogen recovered in the permeate zone is inversely proportional to the steam to ethanol ratio for both kinetic models (figure 2**b** and figure 3**b**). This may be due to the dilution of the hydrogen in the reaction zone caused by the excess of steam. It should be noted that any improving of the hydrogen production increases the hydrogen partial pressure in the reaction zone, which makes an important driving force for hydrogen pumping from the reaction zone to the permeation area. The maximum quantities of hydrogen recovered were in the order of 0.60 and 1.60 for Ni/Mg-Al and Ni/Al_2O_3 kinetic models, respectively. These best performances are obtained at 665 K and with an initial charge of steam to ethanol molar ratio of unity.

In a second step, the optimum values of temperature and of steam to ethanol ratio obtained previously are used in the following for each kinetic. Therefore, the reactor behavior is concretized when a parameter of the permeation zone which is the sweeping gas (I) and another from the reaction zone which is the total pressure (P_t) were manipulated simultaneously, while the pressure in the permeate zone is regulated to the atmospheric level (P_p = 1 atm).

The main results obtained for the two kinetic models show that the production of hydrogen (figure 4**a** and figure 5**a**) was maximum for a minimum values of I and P_t. For both kinetics, the amount of hydrogen recovered was maximal for the maximum values of (I) and (P_t). These quantities are of the order of 0.80 and 2.77 for Ni/Mg-Al and Ni/Al_2O_3 kinetic models, respectively (figure 4**b** and figure 5**b**).

The increase of the sweeping gas ratio can reduce the hydrogen pressure in the permeate zone and creates a driving force promoting the permeation of hydrogen which causes the decrease of the amount of hydrogen in the reaction area and increasing the amount of the recovered hydrogen. The production of hydrogen is inversely proportional to the inert ratio for both kinetic models.

In addition it was found that under the investigated operating conditions, using a small molar flow rate of the sweeping gas was sufficient to shift the equilibrium towards the direction of hydrogen production. This allows minimizing the dilution effect of the recovered hydrogen by the sweep gas. It was found that the total pressure in reaction side has a negative effect on hydrogen production. Increasing pressures allow a decrease in the amount of the produced hydrogen over both catalysts.

Thus, the ethanol steam reforming is favorable by the low pressures according to thermodynamic nature of the involved reactions. In the other hand, increasing total pressure results a high hydrogen partial pressure in the reaction side and stimulates the

driving force and consequently the hydrogen recovery increases with increasing pressure in reaction side.

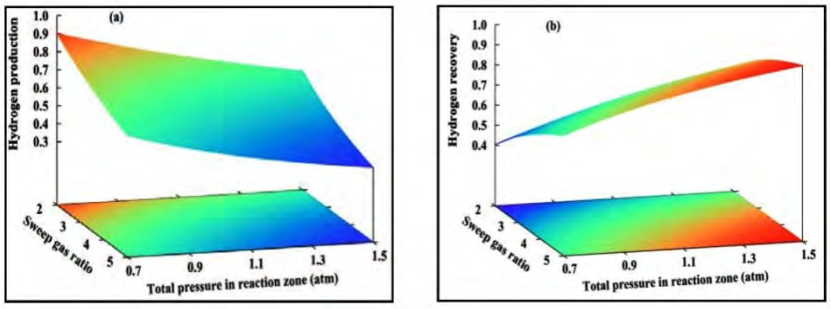

Fig. 4: Effect of the reaction total pressure and sweeping gas ratio on hydrogen production (**a**) and on pure hydrogen recovery (**b**) with Ni/Mg-Al kinetic model

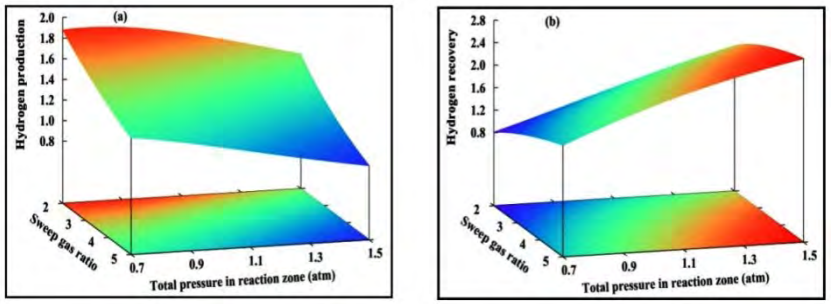

Fig. 5: Effect of the reaction total pressure and sweeping gas ratio on hydrogen production (**a**) and on pure hydrogen recovery (**b**) with Ni/Al_2O_3 kinetic model

Given the important relationship between reaction and permeate pressures, the effect of these parameters are studied simultaneously. The production of hydrogen in the reaction zone is inversely proportional to the reaction total pressure, while it is directly proportional to the permeation pressure for both kinetic models (figure 6**a** and figure 7**a**). This can produce a best correlation between hydrogen partial pressure in permeate side and in reaction side; consequently a synergistic effect between these parameters could be established in favor of hydrogen recovery.

The main results show that the maximum of hydrogen recovery through both kinetic models could be obtained for the small values of permeate pressure, and for high values of total pressure in reaction side (figure 6**b** and figure 7**b**).

The obtained quantity of hydrogen recovered increases with the reaction pressure increase, because of the increase of the driving force between the two sides of the reactor. Increasing the pressure decreases the permeation of the hydrogen to the permeation zone in which causes the accumulation of hydrogen in the reaction zone.

It can be concluded that the imposed low pressures in the permeation zone are favorable to increase the driving force for good hydrogen permeation, and therefore a large amounts of hydrogen could be recovered. Finally, it was obtained that the quantity of hydrogen recovered obtained with the Ni/Al_2O_3 kinetic model is almost three times greater than that obtained by the first one.

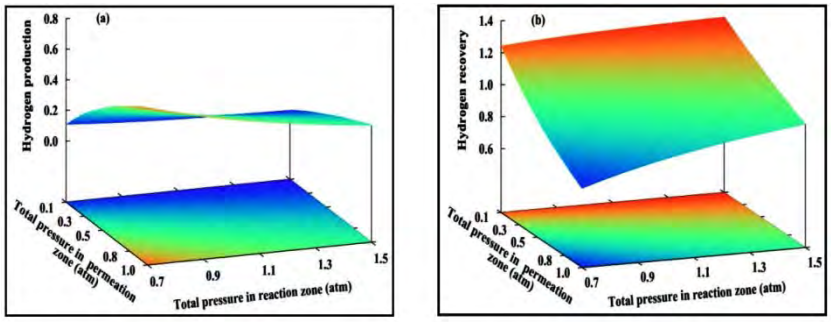

Fig. 6: Effect of the total pressure in both reactor sides on hydrogen production (**a**) and on pure hydrogen recovery (**b**) with Ni/Mg-Al kinetic model

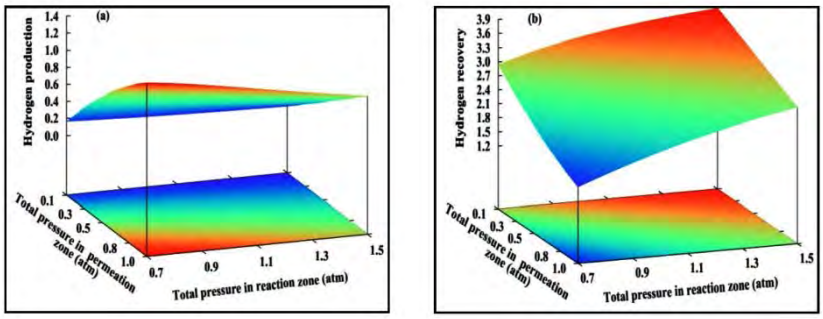

Fig. 7: Effect of the total pressure in both reactor sides on hydrogen production (**a**) and on pure hydrogen recovery (**b**) with Ni/Al_2O_3 kinetic mode

On the other hand, the conversion of ethanol (figure 8) at the optimum conditions was almost complete (100 %) for the Ni/Mg-Al kinetic model and it was nearly total conversion (95 %) for the Ni/Al_2O_3. Since the Ni/Mg-Al kinetic model allows the use of temperatures up to 685 K, the prediction of the ethanol conversion at this temperature was closely 100 % in the reactor exit.

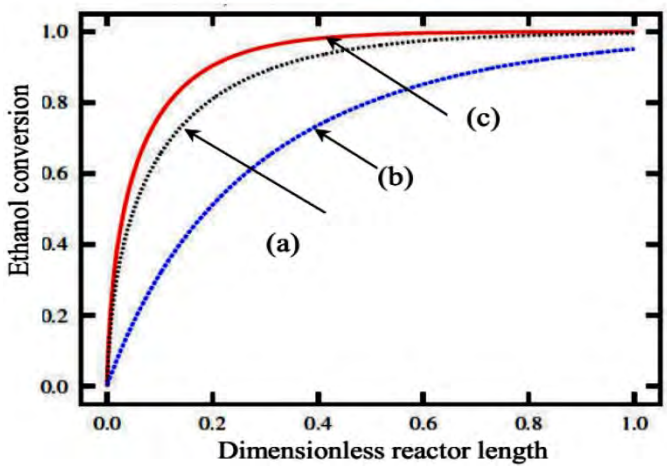

Fig. 8: Ethanol conversion under optimal conditions over Ni/Mg-Al at 665 K (**a**) and at 685 K (**c**) and over Ni/Al_2O_3 at 665 K (**b**)

5. CONCLUSION

Our work is focused to studying the production of pure hydrogen by ethanol steam reforming in a Pd-Ag based membrane reactor, by using two different kinetic models. A parametric sensitivity analysis was conducted to determine the optimal operating conditions leading to maximum hydrogen recovery over Ni/Mg-Al and Ni/ Ni/Al_2O_3 catalysts.

The obtained results show that the performance of the ethanol steam reforming depends strongly both of the used operating parameters and of the used catalyst. The main results show that under the optimal operating conditions the use of the nickel catalyst supported on γ−alumina gives better performance in terms of hydrogen recovery compared to the nickel-based catalyst supported on Mg-Al.

The quantity of hydrogen recovered when using the Ni/Al_2O_3 catalyst was three times greater than that obtained with Ni/Mg-Al catalyst. Furthermore, a quasi-complete conversion of ethanol was achieved when using the Ni/Mg-Al catalyst, while a nearly complete conversion (95%) was obtained with Ni/Al_2O_3 catalyst.

REFERENCES

[1] M. Ball and M. Wietschel, '*The Future of Hydrogen-Opportunities and Challenges*', International Journal of Hydrogen Energy, Vol. 34, N°2, pp. 615 - 627, 2009.

[2] I. Dincer and C. Acar, '*Review and Evaluation Of Hydrogen Production Methods For Better Sustainability*', International Journal of Hydrogen Energy, Vol. 40, N°34, pp. 11094 - 11111, 2015.

[3] L. Chibane, '*Highlighting of the Impact of Periodic Operations on the Performance of Methanol Steam Reforming Process for Pure Hydrogen Generation*', Revue des Energies Renouvelables, Vol. 19, N°4, pp. 663 - 679, 2016.

[4] T. Hou, S. Zhang, Y. Chen, D. Wang and W. Cai, '*Hydrogen Production from Ethanol Reforming: Catalysts and Reaction Mechanism*', Renewable and Sustainable Energy Reviews, Vol. 44, pp. 132 - 148, 2015.

[5] J.A. Calles, A. Carrero, A.J. Vizcaíno and M. Lindo, '*Effect of Ce and Zr Addition to Ni/SiO2 Catalysts for Hydrogen Production Through Ethanol Steam Reforming*', Catalysts, Vol. 5, N°1, pp. 58 -76 , 2015.

[6] J.G.G. Jonker, F. Van Der Hilst, H.M. Junginger, O. Cavalett, M.F. Chagas and A.P.C. Faaij, '*Outlook for Ethanol Production Costs in Brazil up to 2030, for Different Biomass Crops and Industrial Technologies*', Applied Energy, Vol. 147, pp. 593 - 610, 2015.

[7] D. Dionisi, J.A. Anderson, F. Aulenta, A. McCue and G. Paton, '*The Potential of Microbial Processes for Lignocellulosic Biomass Conversion to Ethanol: A Review*', Journal of Chemical Technology and Biotechnology, Vol. 90, N°3, pp. 366 - 383, 2015.

[8] R.M. Navarro, M.C. Álvarez Galván, M.C. Sánchez-Sánchez, F. Rosa and J.L. Fierro, '*Production of Hydrogen by Oxidative Reforming of Ethanol Over Pt Catalysts Supported on Al_2O_3 Modified With Ce and La*', Applied Catalysis B: Environmental, Vol. 55, N°4, pp. 229 - 241, 2005.

[9] J. Sun, X. Qiu, F. Wu, W. Zhu, W. Wang and S. Hao, '*Hydrogen from Steam Reforming of Ethanol in Low and Middle Temperature Range for Fuel Cell*

Application', International Journal of Hydrogen Energy, Vol. 29, N°10, pp. 1075 - 1081, 2004.

[10] R. Rincón, A. Marinas, J. Muñoz, C. Melero, M.D. Calzada, '*Experimental Research on Ethanol-Chemistry Decomposition Routes in a Microwave Plasma Torch for Hydrogen Production*', Chemical Engineering Journal, Vol. 284, pp. 1117 - 1126, 2016.

[11] T. Hou, B. Yu, S. Zhang, T. Xu, D. Wang and W. Cai, '*Hydrogen Production from Ethanol Steam Reforming Over Rh/Ceo2 Catalyst*', Catalysis Communications, Vol. 58, pp. 137 - 140, 2015.

[12] C. Pirez, W. Fang, M. Capron, S. Paul, H. Jobic, F. Dumeignil and L. Jalowiecki-Duhamel, '*Steam Reforming, Partial Oxidation and Oxidative Steam Reforming for Hydrogen Production from Ethanol Over Cerium Nickel Based Oxyhydride Catalyst*', Applied Catalysis A: General, Vol. 518, pp. 78 - 86, 2016.

[13] S. Yun, H. Lim and S.T. Oyama, '*Experimental and Kinetic Studies of the Ethanol Steam Reforming Reaction Equipped with Ultra thin Pd and Pd-Cu Membranes for Improved Conversion and Hydrogen Yield*', Journal of Membrane Science, Vol. 409-410, pp. 222 - 231, 2012.

[14] I. Llera, V. Mas, M.L. Bergamini, M. Laborde and N. Amadeo, '*Bio-Ethanol Steam Reforming on Ni Based Catalyst: Kinetic Study*', Chemical Engineering Science, Vol. 71, pp. 356 - 366, 2012.

[15] F. Gallucci, M. de Falco, S. Tosti, L. Marrelli and A. Basile, '*Ethanol Steam Reforming in a Dense Pd-Ag Membrane Reactor: A Modelling Work. Comparison with the Traditional System*', International Journal of Hydrogen Energy, Vol. 33, N°2, pp. 644 - 651, 2008.

[16] Y.J. Wu, J. Santos, P. Li, J.G. Yu, A.F. Cunha and A.E. Rodrigues, '*Simplified Kinetic Model for Steam Reforming of Ethanol on a Ni/Al2O3 Catalyst*', The Canadian Journal of Chemical Engineering, Vol. 92, N°1, pp. 116 - 130, 2014.

[17] Y.J. Wu, P. Li, J.G. Yu, A.F. Cunha and A.E. Rodrigues, '*Sorption-Enhanced Steam Reforming of Ethanol on NiMgAl Multifunctional Materials: Experimental and Numerical Investigation*', Chemical Engineering Journal, Vol. 231, pp. 36 - 48, 2013.

[18] M. de Souza, G.M. Zanin and F.F. Moraes, '*Parametric Study of Hydrogen Production from Ethanol Steam Reforming in a Membrane Microreactor*', Brazilian Journal of Chemical Engineering, Vol. 30, N°2, pp. 355 - 367, 2013.